- Technical Paper -

LOAD-DISPLACEMENT RESPONSE ANALYSIS FOR COMPOSITE *EWECS* COLUMNS

FAUZAN[*1], Atsuo TAKINO[*2], Kenta SHINDO[*3] and Hiroshi KURAMOTO[*4]

ABSTRACT

This paper presents an analytical study on the seismic behavior of composite EWECS columns which were compared with the experimental data. A moment-curvature analysis based on hysteresis models of materials was conducted to produce the response of the columns subjected to both constant axial load and lateral load reversals. The analytical results showed good agreement with the test data. Moreover, a parametric study using the same numerical model was carried out on columns using double H-section steel to examine the effects of shear-span ratio on behavior of EWECS columns.

Keywords: column, composite structures, fiber section analysis, hysteresis loops, parametric study

1. INTRODUCTION

Engineering Wood Encased Concrete-Steel (EWECS) column is a new composite structural system, which have been developed in recent five years. The columns consist of concrete encased steel (CES) core and an exterior woody shell, as shown in Fig. 1. In this composite column, no mechanical bond or adhesive material was used to connect among each material (steel-concrete-woody shell), however, the natural bond was expected. Structurally, the use of woody shell improves the structural behavior of the column through its action to provide core confinement and resistance to bending moment, shear force and column buckling.

Some experimental studies have been carried out to investigate seismic performance of EWECS columns [1,2]. The results indicated that EWECS columns had excellent hysteretic characteristic and damage limit. In order to compare the test data, furthermore, an analytical study is performed.

This paper presents an analytical study on the seismic behavior of EWECS columns. A moment-curvature analysis based on hysteresis models of materials was conducted to produce the response of the columns subjected to both constant axial load and lateral load reversals. The results of the analytical study were compared with the previous experimental results. A parametric study using the same analytical model was also carried to investigate the effects of shear-span ratio on behavior of the columns using double H-steel.

2. SUMMARY OF TEST PROGRAM

A total of four column specimens of which the scale is about two-fifth, were tested in two test programs, Phases 1 and 2. The dimensions and details of the specimens are shown in Fig. 1 and Table 1. All specimens had a column with 1,600 mm height. In Phase 1, one specimen (Specimen WCS-1) was tested to investigate the seismic behavior of EWECS columns using double H-section steel which was compared with CES column without cover concrete, which corresponds to the core of EWECS column [1]. The column section of Specimen WCS-1 was 400 mm square and the woody shell thickness was 45 mm. Steel encased in the column had a cross-shaped section combining two H-section steels of 300x150x6.5x9 mm.

In Phase 2, three EWECS columns using single H-section steel (Specimens WCS-2, WCS-3 and WCS-4) were tested to investigate the effect of shear-span ratio on seismic behavior of the columns. In this study, the column cross-section was 400 mm square section for all specimens and different shear-span ratios (1.0, 1.5 and 2.0) were achieved by varying the column height (800mm, 1200mm and 1600mm). The steel encased in each column had a single H-section steel of 300x220x10x15 mm and the thickness of the woody shell for all specimens was the same as those of Specimen WCS-1. The mechanical properties of the steel and woody shell used in Phases 1 and 2 are listed in Tables 2 and 3, respectively.

All specimens were loaded lateral cyclic shear forces. The applied axial compression for specimens in Phases 1 and 2 were 770 kN and 1,031 kN, respectively. The axial loads were applied from the top of the stub which is transmitted to the composite column [1,2]. The incremental loading cycles were controlled by story drift angles, R, defined as the ratio of lateral displacements to the column height, δ/h. The lateral load sequence consisted of two cycles to each R of 0.005, 0.01, 0.015, 0.02, 0.03 and 0.04 radians followed by half cycle to R of 0.05 radian.

*1 Postdoct. Researcher, Dept. of Architectural Engineering, Osaka University, Dr.E., JCI Member
*2 Assistant Prof., Dept. of Architectural Engineering, Osaka University. Dr.E.
*3 Senior Researcher, Forestry and Forest Products Research Institute, Dr.E., JCI Member
*4 Prof., Dept. of Architectural Engineering, Osaka University, Dr.E., JCI Member

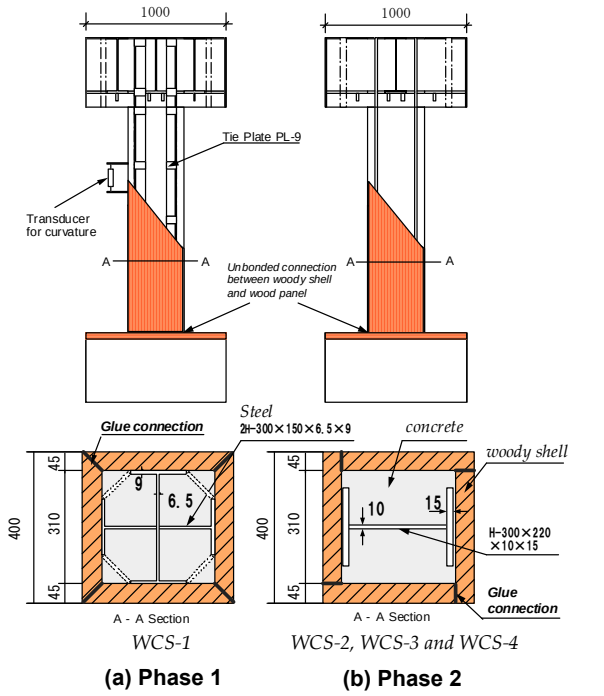

Fig. 1 Test specimen

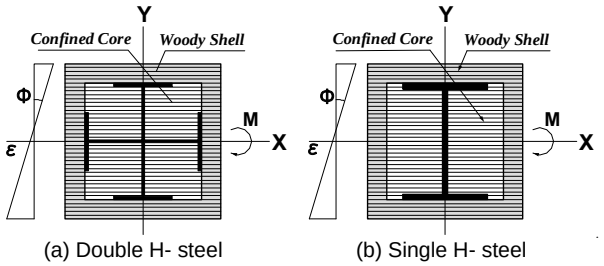

Fig. 2 Fiber model

3. MOMENT CURVATURE ANALYSIS

3.1 Summary of Analytical Method

Fiber section analysis method was used to construct moment-curvature relationships of critical section. In this method, the cross section is discretized into a number of small areas or filaments, as shown in Fig. 2. Each fiber is assumed to be uniaxially stressed and to behave according to assumed stress-strain relationships of its constituting materials, as explained below. As described in the introduction that the natural bond was expected among each material in the composite column. Therefore, the analysis assumed that the plane sections to remain plane, thus implying full compatibility among the steel, concrete and woody shell components of a composite cross-section.

The analysis is controlled through a series of small steps by curvature or displacement history in terms of X-axis. With the axial strain at the center of the cross section, $\Delta\varepsilon_0$ and the curvatures along in terms of X-axis, $\Delta\phi_x$, the axial strain at the fiber element of i, $\Delta\varepsilon_i$ is found according to:

$$\Delta\varepsilon_i = \Delta\varepsilon_0 + y_i \Delta\phi_x \quad (1)$$

where y_i is the distance from the X-axis to the i th fiber element on the section. Considering the equilibrium of the section, axial force ΔN and bending moment ΔM are written as follows, using stiffness matrix [K];

$$\{\Delta N, \Delta M\}^T = [K] \{\Delta\varepsilon_0, \Delta\phi_x\}^T \quad (2)$$

In this analysis, ΔN, ΔM and $\Delta\varepsilon_0$ were calculated by satisfying Eqs. 1 and 2, and considering the mechanical properties of steel, concrete and woody shell, as $\Delta\phi_x$ was the input data.

Considering the experimental results for curvature distribution along the column height [1,2], the relation between curvature and displacement rotation angles, R was assumed as ϕ = 2.3 R/L for Specimens WCS-1 and WCS-2 while for Specimens WCS-3 and WCS-4, it was assumed as ϕ = 1.5 R/L and ϕ = 0.9 R/L, respectively, although in elastic assumption the relation is defined as ϕ = 6 R/L, where L is the column height. The different values in this assumption were due to different shear-span ratios of the analyzed columns in which the maximum curvature of Specimen WSC-4 was around half that of Specimen WCS-2 [2]. In this analysis, the shear rigidity was included in the assumed relationship between ϕ and R.

The hysteretic model used for steel was the trilinear model proposed by Shibata [3], as shown in Fig. 3. The hysteretic models of confined concrete and woody shell adopted were divided linear models shown in Figs. 4 and 5, respectively. No tensile stress was assumed for stress-strain relationships of concrete due to the use of normal concrete (ignore tensile strength). Also, no tensile stress was assumed for stress-strain

Table 1 Test program

Specimen		WCS-1	WCS-2	WCS-3	WCS-4
Shear-span ratio		2.0	2.0	1.5	1.0
Woody Shell Thickness (mm)		45			
Concrete strength (Mpa)		35	27		
Steel	Built-in steel (mm)	2H-300 x 150 x 6.5 x 9	H-300 x 220 x 10 x 15		
	Tie plate (mm)	PL-9	---		
Column Height: h (mm)		1600	1600	1200	800
Cross section : b x D (mm)		400 x 400			
Axial Compression	N (kN)	770	1031		
	N/Ntot	0.14	0.18		
		Phase 1	***Phase 2***		

N_{tot} = total compressive strength of the column

Table 2 Mechanical properties of steel

Steel	Yield Stress σy (MPa)	Max. Stress σs (MPa)	Notes	
2H-300x150x6.5x9	412.5	541.3	Flange	Phase1 (Double H-Steel)
	453	574.8	Web	
PL-9	412.5	541.3	Tie Plate	
H-300x220x10x15	284	450.5	Flange	Phase 2 (Single H-Steel)
	295.5	454.9	Web	

Table 3 Mechanical properties of woody shell

Woody Shell Panel (mm)	Wood type	[a] Comp. Strength σw (MPa)		Elastic Modulus Es (GPa)	
		Phase 1	Phase 2	Phase 1	Phase 2
40x160x4.5	Glue laminated pine wood	36.5	45	10.5	11.5

[a] the direction is parallel to axis of grain

relationships of woody shell because there is no bond at connection (unbonded connection) between woody shell and wood panel attach to stub (see Fig. 1). In the concrete model [4], a magnification factor of concrete strength K for confined core concrete was considered as 1.15 and the compressive strain at the stress peak, ε_0 was taken as 0.0036. For woody shell model, on the other hand, ε_0 was taken as 0.004.

3.2 Analytical Results

Fiber section analysis results were compared with the experimental data for all specimens, as shown in Fig. 6. From this figure, it can be seen that the analytical results for shear force versus story drift responses of the specimens showed good agreement with the test results. The analytical models adequately simulated the behavior of the test specimens. For Specimen WCS-4 with the smallest shear-span ratio, the analytical results agreed well until R of 0.03 rad. The analytical accuracy after R of 0.03 rad. was insufficient because the assumptions were not applicable to experimental situations after this stage due to the significant splitting of woody shell along the column height. In addition, shear deformation was not considered in this analysis. These comparative good results confirmed the accuracy and validity of the proposed numerical analysis to predict the ultimate strength and behavior of EWECS columns under constant axial load and lateral load reversals.

From these comparative good results, moreover, the contribution of each material to shear force and axial load could be analytically examined. Figure 7 shows the contributions of steel, concrete and woody shell to shear force with an increase of story drift for Specimens WCS-1 and WCS-2. As seen in this figure, the steel gave much contribution to shear force for both

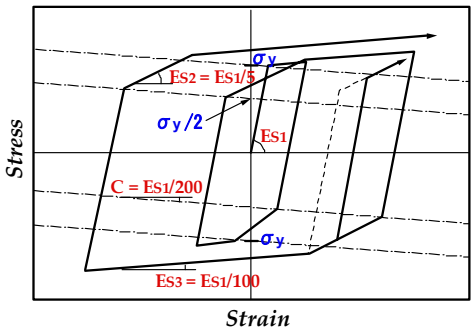

Fig. 3 Stress-strain model of steel

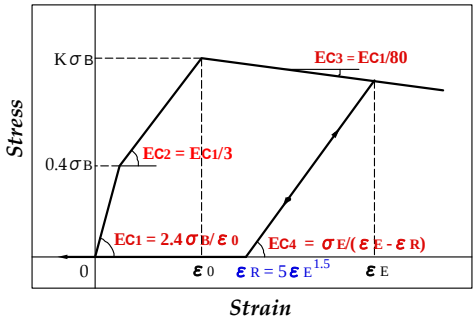

Fig. 4 Stress-strain model of confined concrete

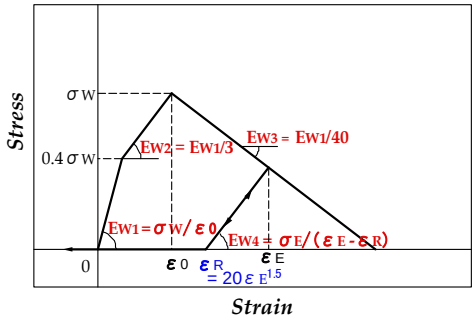

Fig. 5 Stress-strain model of woody shell

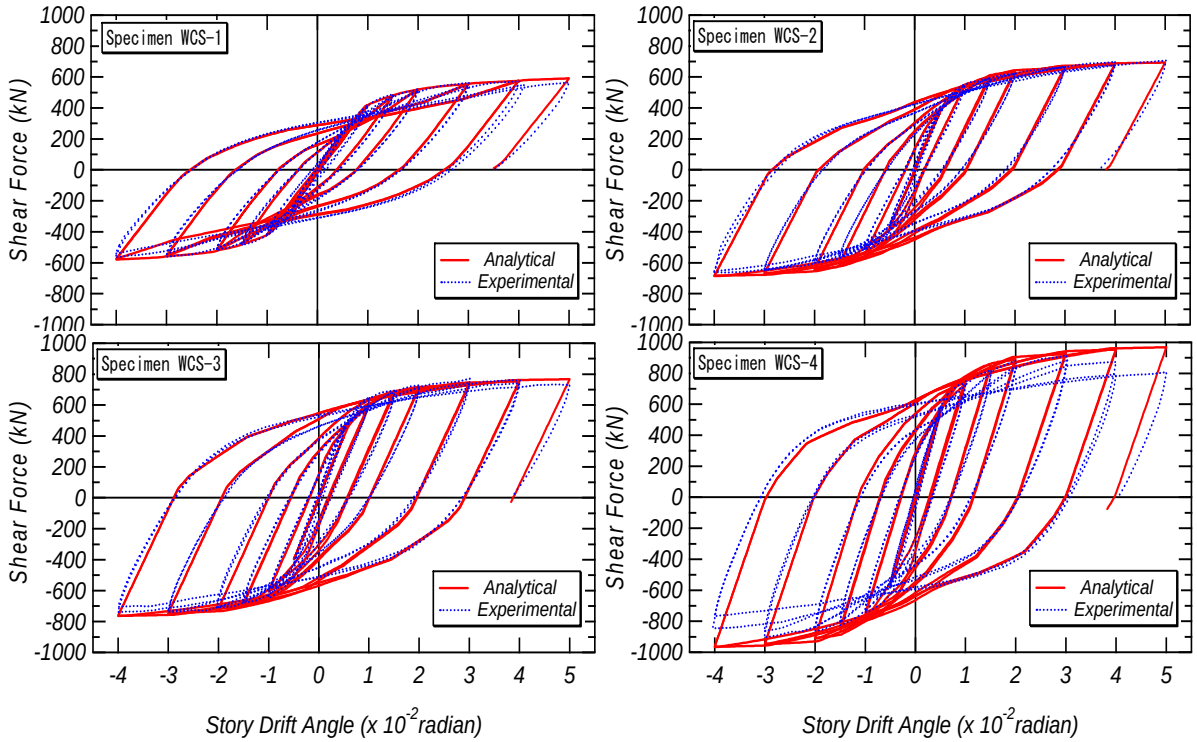

Fig. 6 The comparative results of hysteresis responses for all specimens

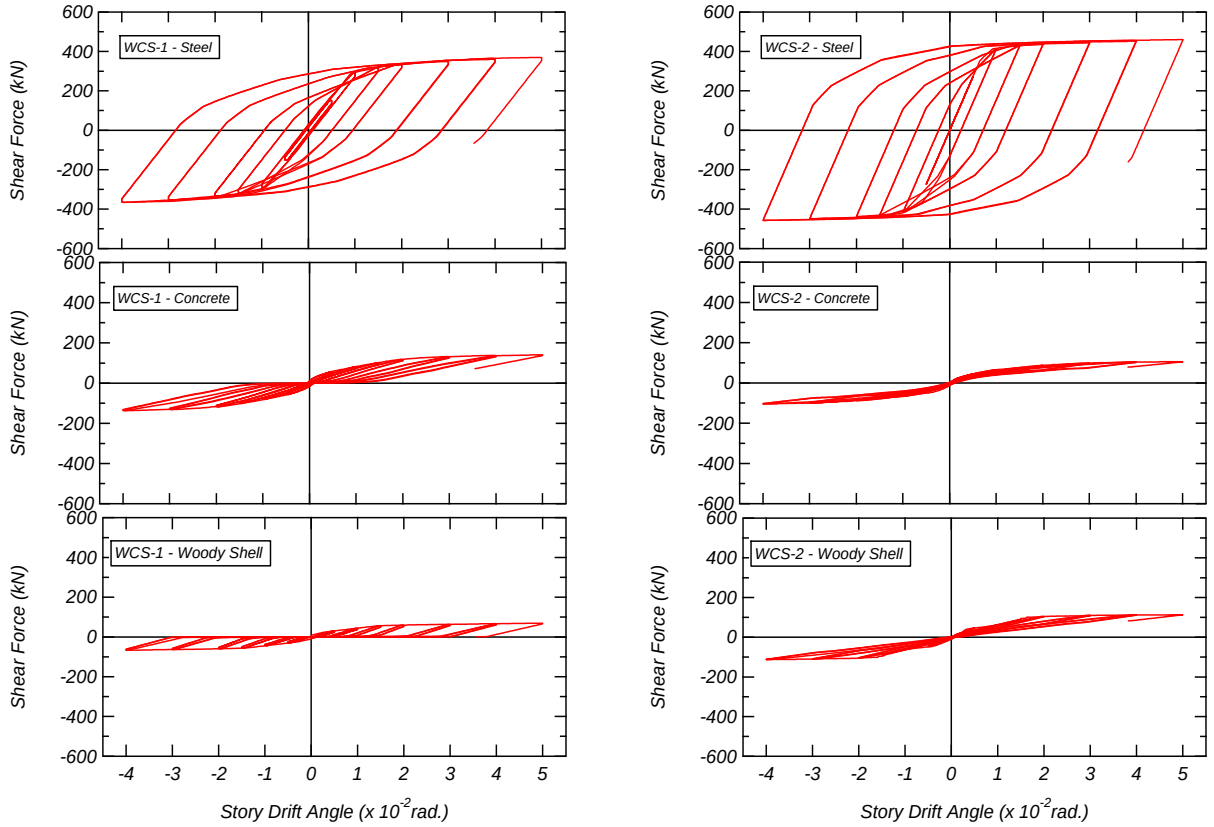

(a) Specimen WCS-1 (Double H-steel)

(b) Specimen WCS-2 (Single H-steel)

Fig. 7 Contributions of each material to shear force

specimens. In Specimen WCS-2, the concrete and woody shell had almost the same contribution value while for Specimen WCS-1, the concrete contribution was higher than the woody shell contribution. The different level of applied axial load and different encased steel used might cause the different distribution pattern of contributions of each material between these two specimens.

From Fig. 7, it can also be seen that the woody shell contributed to the shear force by around 12 % at R of 0.05 rad. for Specimen WCS-1. This result showed a good agreement with the test result in which the maximum capacity of EWECS column increased by around 12 % compared with the capacity of CES column without cover concrete (Specimen CS), which corresponds to the core of EWECS column [1]. It was also found for both specimens that the woody shell contributed to shear force until the maximum R of 0.05 rad., which fully agreed with the experimental results.

The results of this contribution also explained the difference between hysteresis behaviors of EWECS columns using double and single H-steel. From Fig. 6, it is seen that the hysteresis curve of Specimen WCS-2 with single H-steel was more spindle (fat) than that of Specimen WCS-1 with double H-steel. This might be due to the slip that occurred among each material in Specimen WCS-1, as shown in Fig. 7 that the slip appeared in concrete and woody shell curve which might reduce the spindle shape of steel curve, and consequently affected the hysteresis curve of the column.

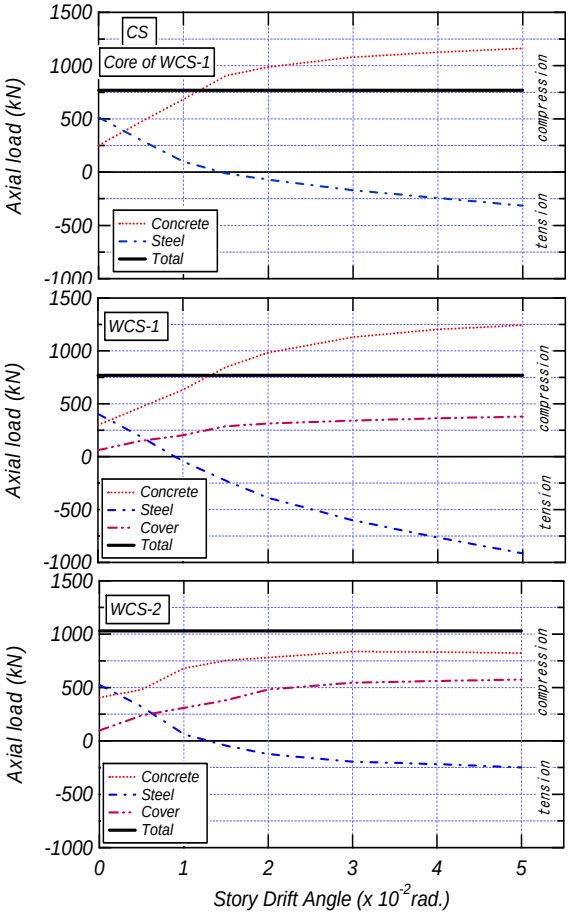

Fig. 8 Contributions of woody shell, concrete and steel to resist axial load

The contributions of steel, concrete and woody shell to resist axial load at each story drift are presented in Fig. 8. In this figure, the analytical result of Specimen CS (the core of Specimen WCS-1) was used as a reference. It is revealed from this figure that the concrete contributed mostly to resist the axial compression, while the steel contributed to the tension. Compared with Specimen CS, the concrete contribution of Specimen WCS-1 to axial compression slightly increased, but the steel contribution to the tension significantly increased due to the additional contribution of woody shell to the axial compression.

The contributions of each material to axial load for Specimen WCS-2 can also be seen in Fig. 8. The patterns of the contributions for this specimen were almost similar with those for Specimen WCS-1, in which the concrete and woody shell contributed only on compression, while the steel contributed to the tension. However, a different distribution pattern was observed on the incremental contributions of each material with the increase of story drift angle. The increase of steel contribution in tension and concrete contribution in compression for Specimen WCS-1 was more significant than those for Specimen WCS-2 while the incremental contribution of woody shell for Specimen WCS-2 was higher than that for Specimen WCS-1. From Fig. 8, it is also seen for Specimens WCS-1 and WCS-2 that the woody shell contributed to axial load until R of 0.05 rad., which agreed with the test results.

4. PARAMETRIC STUDY

Based on the good comparative results between the analytical results and the experimental data, a parametric study has been conducted using the proposed analytical model to investigate the effects of shear-span ratios on the behavior of EWECS columns using double H-steel. Table 4 shows the parameter of shear-span ratio for the columns where the dimension and configurations of the specimens were similar to those of Specimen WCS-1. The ratios of shear-span analyzed were 1.0, 1.5 and 2.0, which were similar to those of the ratios of columns with single H-steel. The analysis results of Specimen WCS-1 were used as reference in this parametric study.

Figure 9 shows the analytical results of hysteresis loops for columns using double H-steel with different shear-span ratios. From this figure, it can be seen that the column strengths significantly increased with decreasing the shear-span ratio. The increase of strength was proportional to the shear-span ratio, where the strength of Specimen WCS-C with shear-span ratio of 1.0 was about 2 times that of Specimen WCS-A with a shear-span ratio of 2.0. This result was different with the columns using single H-steel where the increase of strength due to the decrease of shear-span ratio from 2.0 to 1.0 was about 1.5 times (see Fig. 6). In addition, it was found that the columns using double H-steel had less spindle shape curve for smaller shear-span ratios compared with columns using single H-steel with the same shear-span ratio (Figs. 6 and 9). This indicates that the shear-span ratio has a significant

Table 4 Parameter of shear-span ratio

Specimen	Column height (mm)	Shear-Span ratio	Note
WCS-A	1600	2.0	Specimen configurations are the same as Specimen WCS-1 (Double H-steel)
WCS-B	1200	1.5	
WCS-C	800	1.0	

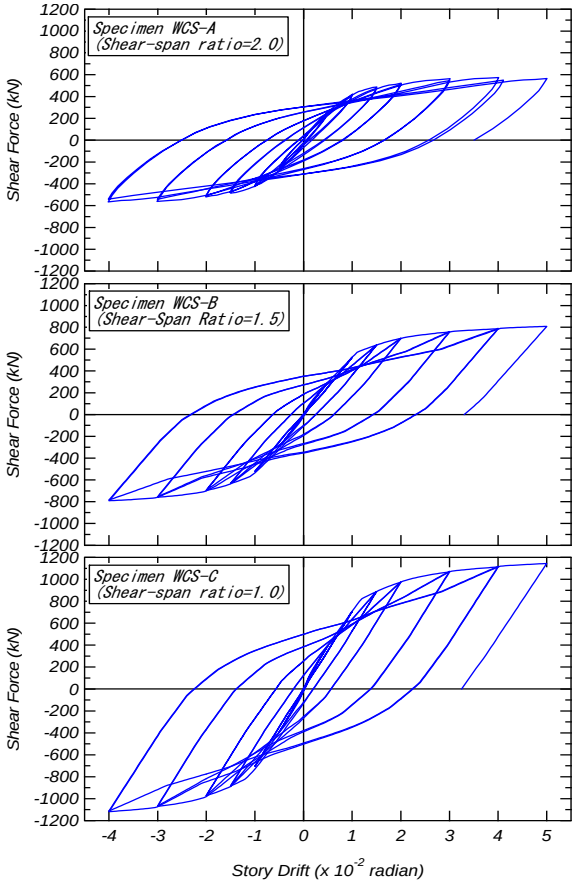

Fig. 9 Hysteresis loops from parametric study

influence not only to the flexural strength of the column but also to the spindle shape of its hysteresis behavior.

Figures 10 and 11 compare the contributions of each material to shear force and axial load for columns with smallest shear-span ratio (shear-span ratio = 1.0), Specimens WCS-C from parametric study and WCS-4. From Fig. 10, it can be seen that the distribution patterns of contribution of each material to shear force for both specimens was almost similar to those of columns with higher shear-span ratio (Fig. 7). As mentioned above that the decrease of shear-span ratio resulted in the increase of maximum strength. This can also be seen from Figs. 7 and 10 that the contribution of each material increased due to the decrease of shear-span ratio. It is also clearly seen from Fig. 10 that the contribution of steel for column with single H-steel was more spindle (fat) than that of column with double H-steel in columns with smaller shear-span ratio.

The distribution patterns of contribution of each material to resist axial load for columns with smallest shear-span ratio were also almost similar to those for columns with higher shear-span ratio (Fig. 8 and 11). The decrease of shear-span ratio resulted in a decrease of contribution of each material to axial load. From Fig.

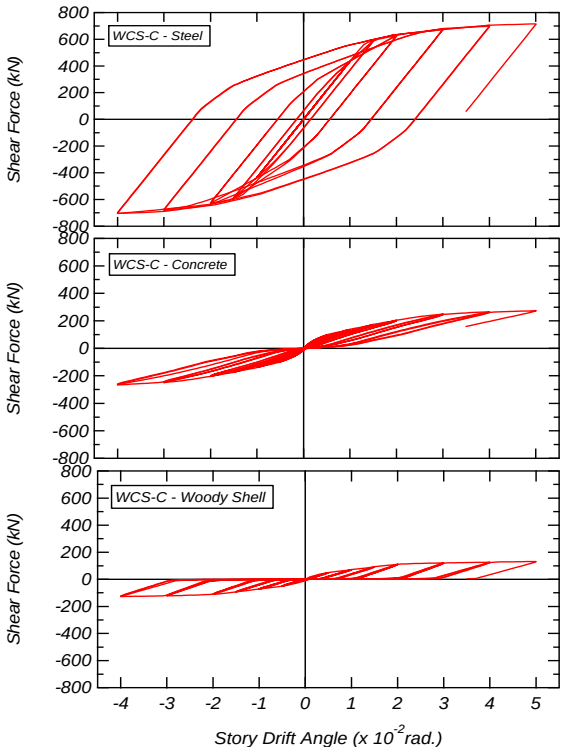

(a) Specimen WCS- C (Double H-Steel)

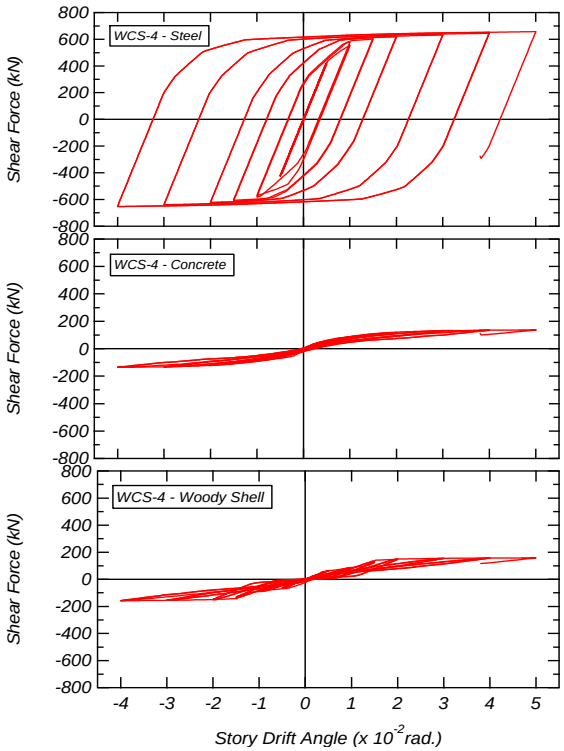

(b) Specimen WCS-4 (Single H-Steel)

Fig. 10 Contributions of each material to shear force for columns with smallest shear-span ratio (1.0)

11, it is also seen that the incremental contributions of concrete and steel with the increase of story drift angle for Specimen WCS-C were more significant than those for Specimen WCS-4 while the woody shell contribution had almost similar incremental contribution for both specimens.

5. CONCLUSIONS

1. The calculated hysteresis loops using fiber section analysis showed good agreement with the experimental results, indicating that the analytical method can be used to predict accurately the ultimate strength and behavior of EWECS columns.
2. The analytical results confirmed the test data for the contributions of woody shell to flexural capacity by around 12 % in maximum. The results also demonstrated the contribution of woody shell to shear force and axial load until R of 0.05 rad.
3. The analytical results found that the slip behavior on concrete and woody shell affects the spindle shape of hysteresis curve for columns with double H-steel.
4. The parametric study results indicated that the shear-span ratio has a significant influence not only to the flexural strength but also to the spindle shape of hysteresis loops for EWECS columns with different encased steel sections.

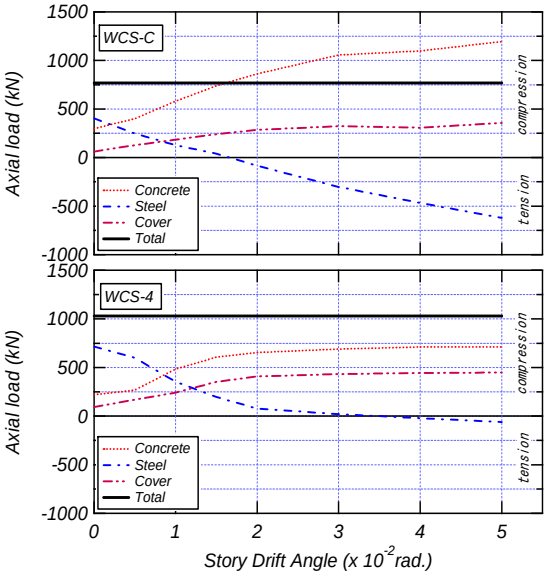

Fig. 11 Contributions of each material to resist axial load for columns with smallest shear span ratio

REFERENCES

[1] Fauzan, Kuramoto, H., Shibayama, Y. and Yamamoto, T., "Structural Behavior of Engineering Wood Encased Concrete-Steel Composite Columns," Proceedings of the Japan Concrete Institute (JCI), Vol.26, No.2, 2004, pp. 295-300.

[2] Fauzan, Kuramoto, H. Matsui, T and Kim, K-H., "Seismic Behavior of Composite EWECS Columns with Varying Shear-Span Ratios", Proceedings of JCI, Vol. 28, No. 2, 2006, pp. 1357-1362.

[3] Shibata M, "Analysisz of Elastic-Plastic Behavior of Steel Brace Subjected to Repeated Axial force", Int. Journal of Solids and Structures, Vol. 8, No. 3, 1982, pp. 217-228.

[4] Kuramoto H., Kabeyasawa T. and Shen F-H., "Influence of axial deformation on ductility of high-strength reinforced concrete columns under varying triaxial forces", *ACI Structural Journal*, Vol. 92 No. 5, 1995, pp. 610-618.